UNIVERSIDADE FEDERAL DO RIO GRANDE DO SUL
INSTITUTO DE CIÊNCIA E TECNOLOGIA DE ALIMENTOS
FACULDADE DE FARMÁCIA
TRABALHO DE CONCLUSÃO DE CURSO DE FARMÁCIA

Nanoencapsulation of linseed oil loaded in chia mucilage as wall material: characterization and its usage in the enrichment of orange juice

Fernanda da Silva Stefani

Orientadora: Prof Dra Simone Hickmann Flôres
Co-orientadora: MSc. Camila de Campo

Porto Alegre,
2017.

APRESENTAÇÃO

Este trabalho está apresentado sob a forma de artigo científico, contendo os seguintes tópicos: Introdução, Material e Métodos, Resultados e Discussão, Conclusão e Referências. Os experimentos foram realizados no Instituto de Ciência e Tecnologia de Alimentos (ICTA) no Laboratório de Compostos Bioativos da Universidade Federal do Rio Grande do Sul (UFRGS), Porto Alegre, Rio Grande do Sul.

Nanoencapsulation of linseed oil loaded in chia mucilage as wall material: characterization, stability and its usage in the enrichment of orange juice

Fernanda da Silva Stefani[a], Camila de Campo[b], Karina Paese[a], Silvia Stanisçuaski Guterres[a], Tania Maria Haas Costa[c]. Simone Hickmann Flôres[b].

[a] *Faculdade de Farmácia, Universidade Federal do Rio Grande do Sul (UFRGS), Av. Ipiranga, 2752, 90610-000, Porto Alegre, RS, Brasil.*
[b] *Instituto de Ciência e Tecnologia de Alimentos, Universidade Federal do Rio Grande do Sul (UFRGS), Av. Bento Gonçalves, n. 9500, CEP 91501-970 Porto Alegre, RS, Brazil*
[c] *Instituto de Química, Universidade Federal do Rio Grande do Sul (UFRGS), Av. Bento Gonçalves, n. 9500, CEP 91501-970 Porto Alegre, RS, Brazil*

Abstract

Omega-3 polyunsaturated fatty acids (Ↄ3-PUFA) have a wide of health benefits, however, its low intake in the western diet and its high oxidation power revealed the need to develop new technologies to supplementation and to decrease the oil oxidation process. In this work, linseed oil (LO) was nanoencapsulated using chia seed mucilage (CSM) as wall material. The nanoparticles were evaluated regarding particle size distribution, zeta potential, pH, span value, viscosity, encapsulation efficiency, loading capacity, transmission electron microscopy, FT-IR and thermal properties. The nanoparticles suspension was spray-dried and the powder was used for the enrichment of orange juice, and sensory evaluation was performed. Nanoparticles in solution presented an average size of 356 ± 2.83 nm, and zeta potential of – 22.75 ± 3.89 mV. The linseed oil nanoparticles (LO-NP) showed spherical shape with encapsulation efficiency of 50 %, loading capacity of 21.37 % and the interaction between linseed oil and chia seed mucilage was evidenced by FT-IR. The thermal analisys showed that LO-NP and CSM were thermally stable up to 300 ºC, suggesting that CSM has satisfactory thermal behavior to be used as wall material. The orange juice had 83 % of overall acceptance and no siginificant difference was observed between orange juice and orange juice with LO-NP. The obtained results suggest that CSM can be used to nanoencapsulate hydrophobic compounds like Ↄ 3-PUFA, increasing its solubility, and spray-dried LO-NP can be used in the enrichment of orange juice.

Keywords: Nanoparticles, Linseed oil, *Linum usitatissimum* L., Chia mucilage, Gum wall, Spray-drying.

1. Introduction

Omega-3 polyunsaturated fatty acids (Ↄ3-PUFA), like docosahexaenoic acid (DHA) and eicosapentaenoic acid (EPA), have a range of food and pharmacological applications, and are also dietary fats with an industrial/commercial interest due to their potential health benefits such as an anti-inflammatory agent (Baboota et al., 2012) and protection from heart attacks by decreasing cardiovascular risk factors (Dawczynski, Martin, Wagner, & Jahreis, 2010).

The Food and Agriculture Organization of the United Nations (FAO, 2010) recommends the intake of 250 mg/day of EPA and DHA combined for vascular health. In many countries where a western style diet is predominant, the intake of EPA and DHA might be below the recommended due to low seafood consumption. For this reason, an interesting application would be to have the Ↄ3-PUFA obtained from vegetable source added into food products. However, due to the low water-solubility and chemical instability, the oil cannot be simply incorporated directly in any food.

Linseed oil, rich in omega-3 (53.21 %), is extracted from the *Linum usitatissimum* L. seeds (Popa et al., 2012). It easily undergoes oxidation as they are unsaturated fatty acids, unstable when exposed to heat, light, moisture, and oxygen and this oxidation can lead to the formation of off-flavor compounds (Kolanowski & Weißbrodt, 2007) and toxic products (Guillén & Ruiz, 2005).

The nanoencapsulation process has been shown to be a good technological alternative to increase oil solubility (Butt et al., 2003), provide protection to the core against volatilization (Flores et al., 2011), delay of auto-oxidation, mask of taste and odor that could be observed in the final product and protection against hydrolysis (Matsuno & Adachi, 1993)

The wall material utilized in nanoencapsulation process, can be obtained from natural or synthetic polymers and the interest in develop natural polymers has been increasing due

to their nontoxic properties and lower costs when compared to synthetic polymers (Prajapati, Jani, Moradiya, & Randeria, 2013). Biodegradable nanoparticles have been shown as a great alternative to increase the stability and solubility of vegetable oils (Martínez et al., 2015). In this context, chia seed mucilage (CSM) has been used as a natural polymer and presented satisfactory behavior as wall material (Bustamante, Oomah, Rubilar, & Shene, 2017; de Campo et al., 2017; Timilsena, Wang, Adhikari, & Adhikari, 2016).

In order to facilitate the nanoparticles application, the production of a powder by spray-drying has been shown a good alternative. Spray-drying is rather an inexpensive and straight forward technique that involves the atomization of suspensions into a drying medium using high temperature and has been used in the food industry for decades (Gouin, 2004).

There are few studies about oil protection against oxidation by nanoencapsulation using natural gums as wall materials (de Campo et al., 2017; Herculano, de Paula, de Figueiredo, Dias, & Pereira, 2015; Ilyasoglu & El, 2014) and enrichment of non-fatty food with these nanoencapsulated oils (Ilyasoglu & El, 2014). Therefore, there is a high demand for the deepening studies in the development of stable nanoencapsulated systems where oils rich in omega-3 could be used to enrich non-fatty foods so that they are enriched with omega-3.

This work aimed to prepare and to characterize linseed oil nanoparticles (LO-NP) using chia seed mucilage (CSM) as wall material, in order to increase the oil water-solubility and protect against degradation. Furthermore, to evaluate its food application, a nanoparticle powder was produced and applied in orange juice and evaluated sensorially.

2. Material and methods

2.1 Material

Linseed oil (LO) was purchased from Pazze and orange juice from Naturale® in a local market (Porto Alegre, Brazil) and stored at 10 ºC. Chia seed mucilage (CSM) was extracted from chia seeds by the method described by (Dick et al., 2015). Ethanol and Tween 80® were provided by Dinamica® (São Paulo, Brazil), acetic acid by Neon® (São Paulo, Brazil)

and mannitol by Delaware® (Porto Alegre, Brazil). All the other reagents, chemicals and solvents utilized were of analytical grade.

2.2 Preparation of CSM solution

The dried CSM was slowly dissolved in distilled water (0.1 % w/v) under stirring with an eletric stirrer (Edutec, EEQ9034, Curitiba, Brazil) for 4 hours at room temperature (25 ºC) to ensure a homogeneous dispersion. The solution was kept overnight under refrigeration at 10 ºC to full hydration, and then was filtered to remove any interfering remained particles. The pH was adjusted to 4 with acetic acid 1N.

2.3 Preparation of LO-NP in suspension

Linseed oil nanoparticles were produced from the method described by (Herculano et al., 2015) with modifications. The organic phase was obtained by adding Tween 80® (13.5 mg), and LO (25 mg) in ethanol under stirring in a magnetic stirrer (Fisatom, model 752A, Brazil) for 15 min at room temperature (25 ºC) until complete dissolution. The organic phase was added dropwise in 20 ml of the previously prepared CSM solution during homogenization in Ultra Turrax (IKA Ultra Turrax digital, model T25, Germany) for 15 min at 8000 rpm. The resulting emulsion was stored at 10 ºC until the spray-drying process.

2.4 Characterization of LO-NP

2.4.1 Hydrogen Potential (pH)

The pH of the LO-NP suspension was performed at 25 ºC using a potentiometer (Quimis®, model Q-400A0, Diadema, Brazil).

2.4.2 Zeta potential

The zeta potential was measured at 25 ºC through of electrophoretic mobility of the nanoparticles in suspension (Zetasizer Nano ZS®, Malvern, UK), using 0.1 M NaCl as dispersant (1:40 v/v) and the results were analyzed by Zetasizer 7.11 program.

2.4.3 Viscosity

The apparent viscosity of the suspension was determined in a rotational viscosimeter (Brookfield®, model DV+II Pro, sprindle LV2, Brookfield Engineering, USA) at 25 ºC just after LO-NP preparation. Brookfield Rheocalc 32 software was used to analyze the results.

2.4.4 Particle size distribution

The volume-weighted mean diameter ($D_{4,3}$) and homogeneity of distribution expressed by span value were measured by laser diffraction (LD Mastersizer 2000 5.61, Malvern Instruments, UK) with water as dispersant. The refractive indexes used for water and CSM were 1.330 and 1.335, respectively. Mastersizer 2000 5.61 software® was used to analyze the results.

2.4.5 Transmission electron microscopy (TEM)

The morphological analysis was performed by Transmission Electron Microscopy (TEM). The LO-NP samples were diluted in ultrapure water (1:10 v/v), transferred to an eppendorf that and kept in water bath in an ultrasom for 5 min. After that, 2 drops of the dilution was dispersed on a grid (Formvar-carbon support films 400 mesh) and after 5 min, a drop of uranyl-acetate (2 % w/v) was also deposited. The analysis was performed in TEM (Jeol, JEM 1200 Exll, Electron Microscopy Center, UFRGS, Brazil) operated at 80 Kv with magnifications of 200x.

2.4.6 Thermal analysis

The thermal characteristics of CSM and LO-NP were performed using a differential scanning calorimeter (PerkinElmer, model DSC 8500, Massachusetts, United States) under heating rate of 10 °C/min^{-1} at temperature range of 25 to 400 °C and a thermogravimeter analyzer (PerkinElmer , model Pyris 1 TGA, Massachusetts, United States) performed

under nitrogen atmosphere, utilizing heating rate of 10 °C/min^{-1}, at temperature range of 25 to 850 ºC.

2.4.7 Fourier transform infrared spectroscopy (FT-IR)

The LO, CSM, and LO-NP were characterized by Fourier transform infrared spectroscopy (FT-IR) using KBr pellets in a spectrophotometer (Shimadzu, model IRPRESTIGE-21, Japan), in the transmittance mode, using wavenumbers between 400 – 4000 cm^{-1}, and 32 scans with a resolutioon of 4 cm^{-1}.

2.4.8 Fatty acids profile

The fatty acid methyl esters (FAME) of LO were quantified by gas chromatography using GC-FID (SHIMADZU, model GC- 2010 Plus, Japan). The FAMEs were identified with a fused silica capillary column SLB-IL 100, Supelco® analytical (30 m x 0.25 mm x 0.2 µm). The CG-FID was equipped with an automatic injector and flame ionization detector coupled. The initial column temperature was kept at 50 °C for 3 min and then was increased to 240 °C at the rate of 3 °C/min. The volume injected was 1 µL and hydrogen was used as carrier gas (20 cm/s) at a flow rate of 1mL/min and split ratio 1:50. The data were processed using GC-Real time data processor (Shimadzu Corporation, Columbia, MD).

To determine the total oil content nanoencapsulated, LO was extracted from LO-NP through the method described by Timilsena et al. (2016). To nanoparticle rupture, 4 N hydrochloric acid (40 mL) was added to 20 ml of LO-NP and mixed in a vortex (IKA® vortex, model VG 3S32, USA) for 1 min. Then, hexane (20 ml) was added and the solution was kept in a vortex for 1 min. To facilitate the migration of the oil to hexane, the solution was stirred on a shaker (CERTOMAT® shaker, model MO II, Germany) for 4 hours. The solvent phase was separated by washing with NaCl satured solution in a separation funnel and dried in N_2.

The LO was submitted to saponification with a methanolic solution of NaOH 0,5 N before injection. The determination of the fatty acid methyl esters (FAME) content of the oil samples, was performed according to the methodology described by Joseph & Ackman,

(1992). The identification was made by comparison of the retention time with the external standard FAME (FAME MIX Supelco® 37, Sigma- Aldrich, St. Louis, MO, USA). The quantification was made using area normalization. The internal standard was 2,6-di-t-butyl-p-hydroxytoluene (BHT) at concentration of 0.5 mg/ml and results were analyzed by GC solution software program.

2.4.9 Encapsulation efficiency (EE) and loading capacity (LC)

Encapsulation efficiency (EE) was performed through determination of total oil nanoencapsulated and free oil in the surface of nanoparticles using GC-FID. The total oil content was determined after extraction from LO-NP, as cited in item 2.4.8. The free LO content was determined by the method described by (Timilsena et al., 2016) with some modifications. To remove the oil to the solvent phase, hexane (20 ml) was added in LO-NP and kept in a vortex of 1 min. The solvent phase was separated in a separation funnel and dried in N_2. FAME MIX was used as external standard to comparison of retention time, and BHT was utilized as internal standard. EE (%) was determined according to the following equation:

$$E.E\ (\%) = \frac{TO-EO}{TO}\ x\ 100 \qquad \text{Eq. (2)}$$

Where: TO is the total fatty acid methyl esters content in LO extracted from nanoparticles and EO is the fatty acid methyl esters content (mg/100g) of free LO in aqueous phase.

LC (%) was calculated according to Eq. (3):

$$\text{LC}\ (\%) = \frac{Total\ amount\ of\ loaded\ LO}{Mass\ of\ nanoparticles\ constituents}\ x\ 100 \qquad \text{Eq. (3)}$$

2.5 Preparation of spray-dried LO-NP

To facilitate the application of nanoparticles in orange juice, the LO-NP suspension was subsequently turned into a powder by spray-drying using mannitol 5 % (w/v) as drying adjuvant, added to the suspension under magnetic stirring for 10 min. The nanoparticles powder were obtained in triplicate in a laboratory-scale Mini Spray Dryer B-290 (Buchi, Switzerland) operating at inlet temperature of 160 ºC, outlet temperature of approximately 92 ºC, air volume flow of 60 L/h, aspirator flow of 35 m^3/h (100 %) and pump feed flow of 5 ml/min (18 %). The yield (%) was calculated as the ratio between the total mass of the powder collected and the total dry mass of the components.

Redispersion efficiency (RE) is based on treatment temperature and time and evaluates the reverse agglomeration behavior (Duan et al., 2016). The RE of nanoparticles after spray-drying was determined using Eq.4, where closer to one, better is the powder redispersion.

$$RE = d_{RP}/d_S. \text{ Eq. (4)}$$

Where d_{RP} is the mean particle size of the redispersed powder and d_S is the mean particle size of the nanoparticles suspension.

The powder was dispersed in water and measured by laser diffraction (LD) (Mastersizer 2000 5.61, Malvern Instruments, UK). The refractive indexes used for water and CSM were 1.330 and 1.335, respectively. Mastersizer 2000 5.61 software® was used to analyze the results.

2.6 Enrichment of orange juice with LO-NP

The FAO recommends the intake of 250 mg/day of EPA and DHA combined. Based on these recommendation, 100 ml of orange juice were enriched with 1.7 g of spray-dried LO-NP powder (5,8 % of EPA/DHA daily recommendation) and stirred until complete dissolution.

2.7 Characterization of orange juice enriched with LO-NP

2.7.1 Hydrogen potential (pH), total soluble solids (TSS) and titratable acidity (TA)

The orange juice pH was performed at 25 ºC using a potentiometer (Quimis, model Q-400A0, Diadema, Brazil). Total soluble solids were determinated by a digital refractometer (ATAGO®, model PR-100, USA) and titratable acidity (TA) was determined by dilution of 10 ml of orange juice in 90 mL of distilled water, and 25 ml sample of this dilution was titrated with 0.1 N NaOH, using phenolphthalein as indicator. The results were expressed as percentage of citric acid.

2.7.2 Color measurements

A portable colorimeter (Konica Minolta®, model CR 400, Singapore) was used to perform the color measurements. The color determination was based on three color co-ordinates, L* (brightness) a* (red-green intensity) and b* (yellow-blue intensity) (Rocha & Morais, 2003). The instrument was calibrated using a white plate and the color measurements were taken in triplicate.

2.8 Sensory evaluation

To evaluate the sensorial acceptance of orange juice enriched with LO-NP powder, two juice samples, pure orange juice and orange juice with LO-NP powder, were given to 50 untrained judges (18 to 47 years). The samples were evaluated regarding attributes such as appearance, color, texture, taste, flavor, aftertaste, and overall acceptability, using a nine-point hedonic scale ranging from 1 to 9, where 1 means dislike very much and 9 like very much (Meilgaard, Civille, & Caar, 2007). The samples were offered in plastic cups and labeled with three-digit random numbers. The percentage of acceptance of each attribute was calculated with the following equation (Eq.5).

$$\%\, Acceptance = \frac{Average\ acceptance}{9}\ x\ 100 \quad \text{Eq. (5)}$$

2.9 Statistical Analysis

For the analysis of difference between means, ANOVA and Tukey test were applied at a significance level of 5 % by Statistica 12 software (Statsoft Inc.®, São Paulo, Brazil).

3. Results and discussion

3.1 Hydrogen Potential (pH), Zeta potential and Viscosity

The total electric charge on nanoparticles surface is indicated by zeta potential (Dickinson, 2006) through electrophoretic mobility (Gittings & Saville, 1998). The presence of carboxylic acid groups (COO^{-}) in CSM gives negative charges to polymer fraction and indicates a negative zeta potential (Goh et al., 2016). Generally, values between +30 mV and -30 mV produce electrostatic stables systems over time (Wongsagonsup, Shobsngob, Oonkhanond, & Varavinit, 2005). In this study, zeta potential of LO-NP was –22.75 ± 3.89 mV, suggesting electrostatic stability. Similar result ranging between –22 to –25 mV was found by (Sarika, Pavithran, & James, 2015) for cationized gelatin and gum arabic complex nanoparticles (1:1, v/v) at pH 10. Results from –35 to –45 mV have been reported for linseed oil nanoemulsions used to improve paclitaxel efficacy in formulations to overcome multidrug resistance in tumor cells (Ganta & Amiji, 2009). (dos Santos et al., 2015) observed lower zeta potential values (-11.5 ± 0.40 mV) for lycopene-loaded lipid-core nanocapsules using poli-ε-caprolactone (PCL) as wall material.

Regarding to pH, LO-NP presented pH value of 4.0. (Timilsena et al., 2016) reported that zeta potential is influenced by medium pH. They observed when pH is above of 2, negative charge gradually increases, while pH values below of 2 induces positive charges for microcapsules of chia seed oil with chia seed mucilage and chia seed protein as wall material.

The viscosity is the internal resistance of a liquid to flow and this property is important to evaluate stability, and process steps such as mixing and quality control. The viscosity-shear rate curves of LO-NP suspension are shown in Fig 1. As observed, the behavior was typically Newtonian with a linear correlation between shear stress and shear rate, and

presented viscosity of 2.98 ± 0.08 mPa.s at 25 °C. The LO-NP suspension was expected to present Newtonian behavior due to CSM low concentration and interaction between nanoparticles components and hydrocolloids molecules. Similar results were reported by de Campo et al. (2017) that used chia seed gum as wall material at concentration of 0.1 % and exhibited typical Newtonian behavior and viscosity of 3.21 ± 0.15 mPa.s. (Timilsena et al., 2016) used CSM at polymer concentration of 0.1 % and reported pseudoplasticity behavior.

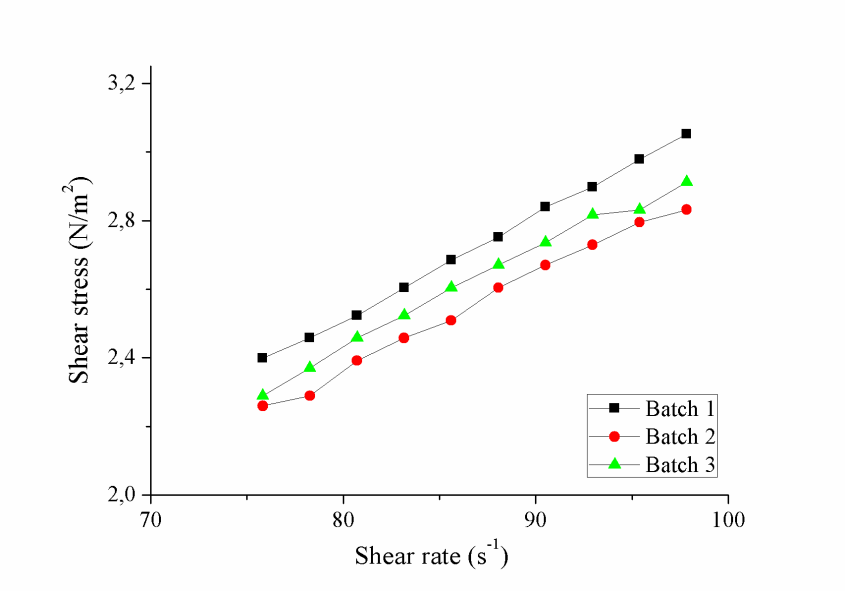

Fig 1. Rheological behavior of LO-NP in triplicate.

3.2 Transmission electronic microscopy (TEM)

The morphology of LO-NP was determined by TEM. Spherical shape, regular distribution, and absence of aggregation were observed (Fig 2). De Campo et al. (2017) studied nanocapsules of chia seed oil with CSM as wall material and observed the same morphological profile.

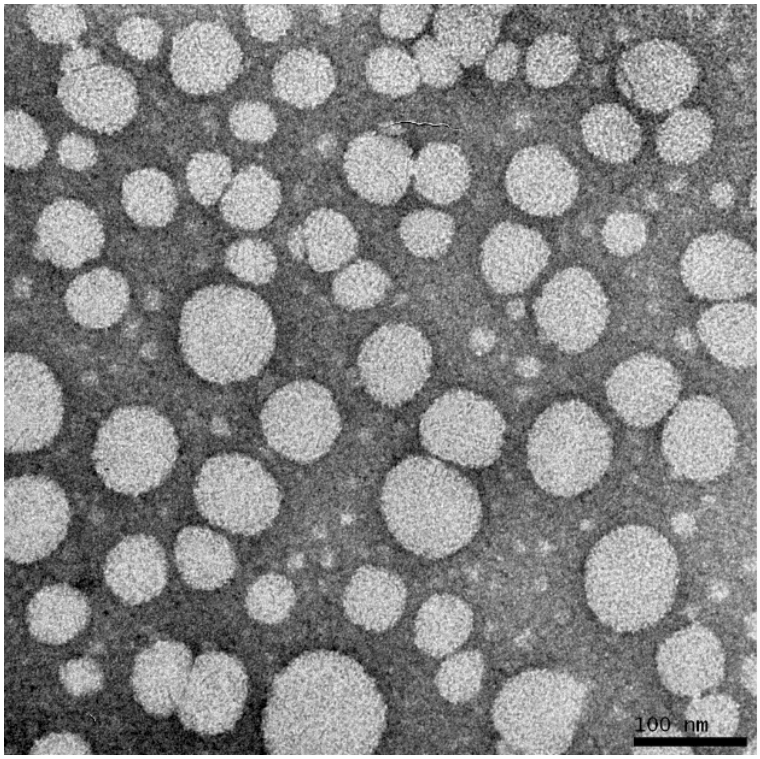

Fig. 2. TEM image of LO-NP at 200x magnification [bar value= 100 nm].

3.3 Thermal Analysis

The thermogravimetric curves shows the thermal stability through sample mass loss and peak temperature for the thermal events. The thermal degradation behavior of CSM and LO-NP are presented in Fig. 3 (a). The gum decomposition shows the presence of four thermal events for CSM and three for LO-NP with temperatures ranging from room temperature (approximately 25 ºC) to 850 ºC. The first event is described as free water loss, where the sample presented evaporation from ~ 25 to 150 ºC representing 12.37 % of water loss for CSM and ~5 % for LO-NP. The following other stages are associated with polysaccharides decomposition from wall material and occurred with the temperature range of ~ 150 to 775 ºC for CSM and ~ 150 to 750 ºC for LO-NP, equivalent to loss of 75.6 % for CSM and 95.36 % for LO-NP. Similar values were reported by (de Campo et al., 2017), where 4 % of water loss for CSM and chia seed oil nanoparticles (CSO-NP) was observed at temperatures ranging from ~ 25 to 150 ºC and losses of 75.6 % for CSM and 82.4 % for CSO-NP are associated with polysaccharides decomposition from wall material at temperatures ranging

from ~ 150 to 770 ºC for CSM and ~ 150 to 790 ºC for CSO-NP. (Khoshakhlagh, Koocheki, Mohebbi, & Allafchian, 2017) observed water losses of 10.62 % from 57 to 177 °C for Alyssum homolocarpum seed gum nanoparticles utilized to encapsulation of d-limonene. The two other steps of weight loss were observed at 242–331 °C (67.86 %) and at at 370–437 °C (16.28 %), associated to a complex process including degradation of the saccharide rings and disintegration of macromolecular chains of gum.

The differential scanning calorimetry of CSM and LO-NP is shown in Fig 3 (b). CSM showed endothermic peak at approximately 100 ºC owing to water loss and LO-NP at 125 ºC. The exothermic events concerning polysaccharide structure decomposition were observed at 300 ºC for CSM and LO-NP. Similar findings were presented by (de Oliveira, Paula, & Paula, 2014) with temperature ranging from 379 to 392 ºC associated to polymer chain decompositions in cashew gum and alginate. TGA and DSC data showed that LO-NP and CSM were thermally stable up to 300 ºC, suggesting that CSM has satisfactory thermal behavior to be used as wall material for nanoparticles, offering protection to the linseed oil against oxidation.

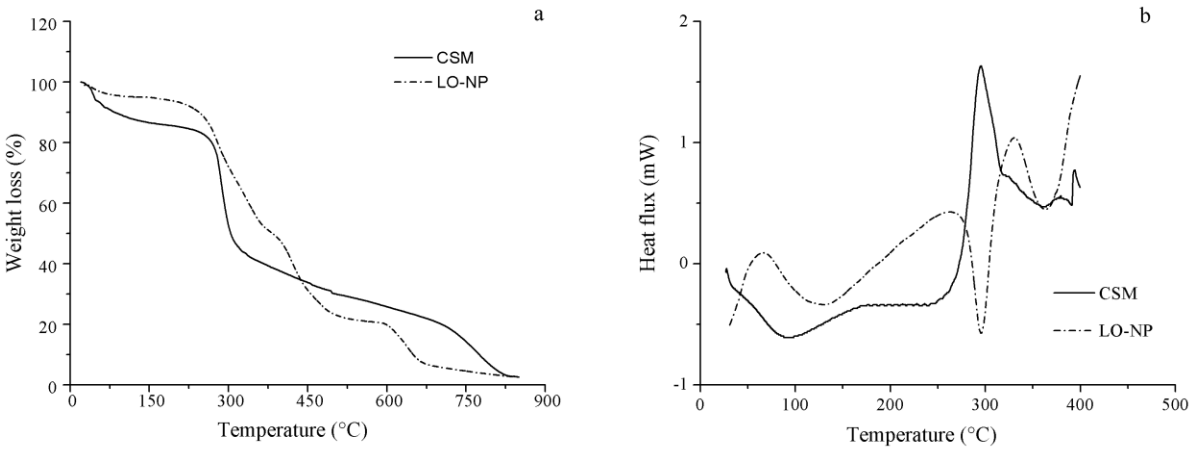

Fig. 3. Thermogravimetric analysis (TGA) (a) and differenntial scanning Calorimetry (DSC) (b) for CSM and LO-NP.

3.4 Fourier transform infrared spectroscopy (FT-IR)

Infrared spectra of CSM, LO and LO-NP can be seen in Fig 4. The LO and CSM interactions causes vibrational absorptions of chemical groups (Silverstein, Webster, &

Kiemle, 2007). The CSM spectra showed a broad band at 1033 cm^{-1}, associated to C-O-C groups vibration, a band at 3334 cm^{-1} assigned to – OH stretching vibration also seen in LO-NP, and a band at 2910 and 2920 cm^{-1} assigned to C-H, also visualized in LO and LO-NP spectra (Goh et al., 2016). The LO and LO-NP infrared spectra revealed overlapping bands at 1743 cm^{-1}corresponding to C=O stretching vibration (Hayes, Vahur, & Leito, 2014).

The bands of CSM at ~1620 and ~1420 cm^{-1} assigns respectively to the peak of mannose (Goh et al., 2016) and to stretching vibration of carboxylic group of uronic acid, which confer anionic characteristics to the macromolecule (Timilsena et al., 2016). Additionally, the peak corresponding to C=O bond (1743 cm^{-1}) presented a significant reduction in LO-NP indicating that the group is involved in bonding between LO and CSM.

CSM, LO and LO-NP have many overlapping bands and presented vibrational absorptions confirming the interaction between CSM and LO and effectiveness of the nanoencapsulation method used to obtain LO-NP.

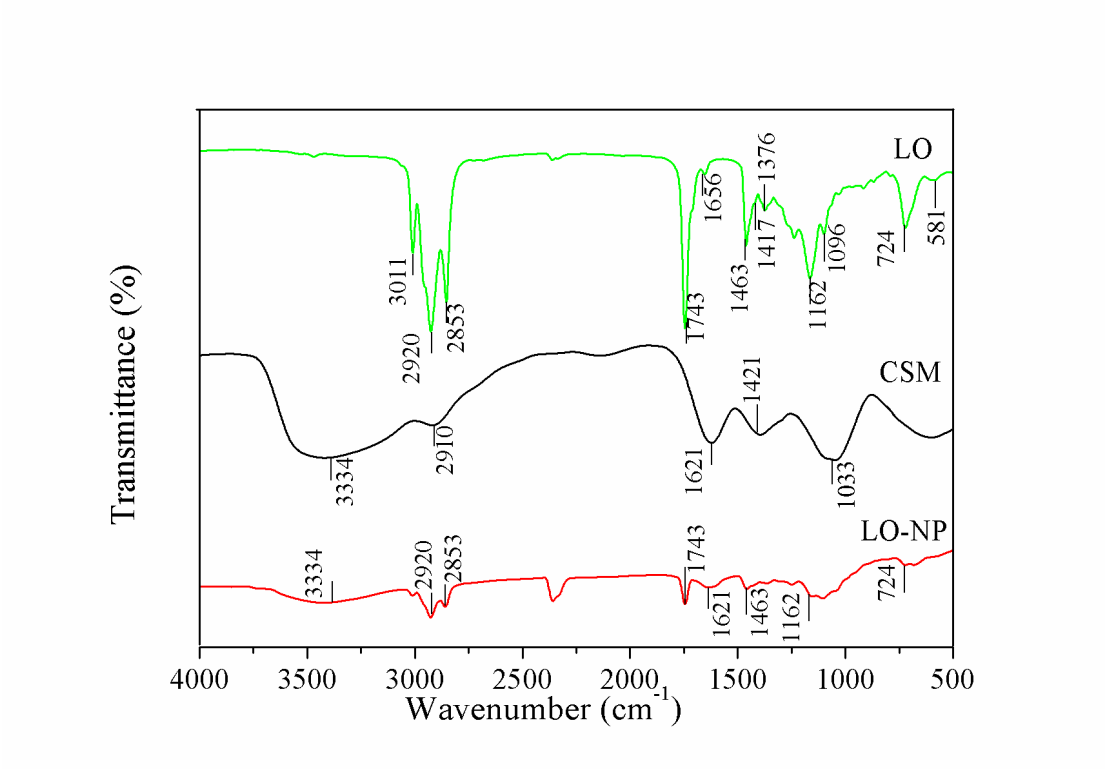

Fig 4.Fourier transform infrared spectroscopy (FT-IR) for CSM, LO and LO-NP.

3.5 Fatty acids profile

The fatty acids profile is shown in Table 1. As observed, unsaturated fatty acids are the main fatty acids (86.37 %) in linseed oil, while saturated fatty acids represented 9.25 %. The main components of unsaturated fatty acids are linolenic acid (54.31 %), oleic acid (20.82 %) and linoleic acid (11.24 %). (Popa et al., 2012) found similar values of 53.21 % of linolenic acid, 18.51 % of oleic acid and 17.25 % of linoleic acid. (El-Beltagi, Salama, & El-Hariri, 2007) found 46 – 50 % of linolenic acid, 22 % of oleic acid and 18.2 % of linoleic acid.

Table 1. Fatty acids profile of linseed oil.

	Content (%)	Retention time
Palmitic Acid (C16:0)	5.46 ± 0.13	11.39
Stearic Acid (C18:0)	3.79 ± 0.14	13.98
Oleic Acid (C18:1n9c)	20.82 ± 0.01	14.36
Linoleic Acid (C18: 2n6c)	11.24 ± 0.03	15.07
α – Linolenic Acid (C18:3n3)	54.31 ± 0.29	16,23

The results are represented as the means ± standard desviation (n = 3).

3.6 Encapsulation efficiency (EE) and loading capacity (LC)

The encapsulation efficiency suggests the adequate oil encapsulation into the wall material. The EE of LO-NP was 50 %. EE in the range of 52.5 to 65.5 % was obtained by (González, Martínez, Paredes, León, & Ribotta, 2016) using soy protein and maltodextrin as wall material of chia oil microcapsules. (Gallardo et al., 2013) had 90 % of EE for linseed oil microencapsulated using gum arabic as wall material prepared by high shear homogenizer that produces emulsions with higher particle size distribution than the ultra-homogenizer Ultra Turrax. The high EE found for LO-NP indicates large amount of oil entrapped in the nanoparticle core.

The loading capacity indicates the proportion of oil amount in relation of all the constituent's amount utilized to nanoparticles obtention. It's a parameter utilized to evaluate the affinity of the lipid core with the wall material. According to the results shown for EE,

nanoparticles presented a LC of 21.37 %. This LC percentage indicates that the method utilized to obtain LO-NP was efficient, due to the oil affinity with CSM. Nanoparticles of BSC-Glutathione loaded in basil seed gum presented lower values of 7 – 13 % (Naji-Tabasi & Razavi, 2017).

*3.7 Spray-dried nanoca*particles

The process yield of spray-dried nanoparticles was 61.00 ± 2 % and the redispersion efficiency was 0.74. Particle size (Fig. 5) was measured immediately after redispersion and compared to the particle size of nanoparticles in suspension. After redispersion, the LO-NP presented a smaller diameter, but remained on the nano-scale with similar profile, evidencing that the LO-NP can be spray-dried, without significant changes in the size distribution profile. The LO-NP nanoparticles suspension presented a particle size distribution of 356 ± 2.83 nm with a span value of 2.62 ± 0.05. Immediately after water redispersion, the average particle size was 262 ± 4.95 nm with a span value of 2.39 ± 0.16. These finding indicates that the spray-drying technique did not induce aggregation and particle size increase. However, indicates that the water content retained by the nanoparticle during the production process affected the diameter when suspension was spray-dried. The loss of water from the wall material during the drying process can induce a decrease in particle size. (Us-Medina, Ruiz-Ruiz, Quintana-Owen, & Segura-Campos, 2017).

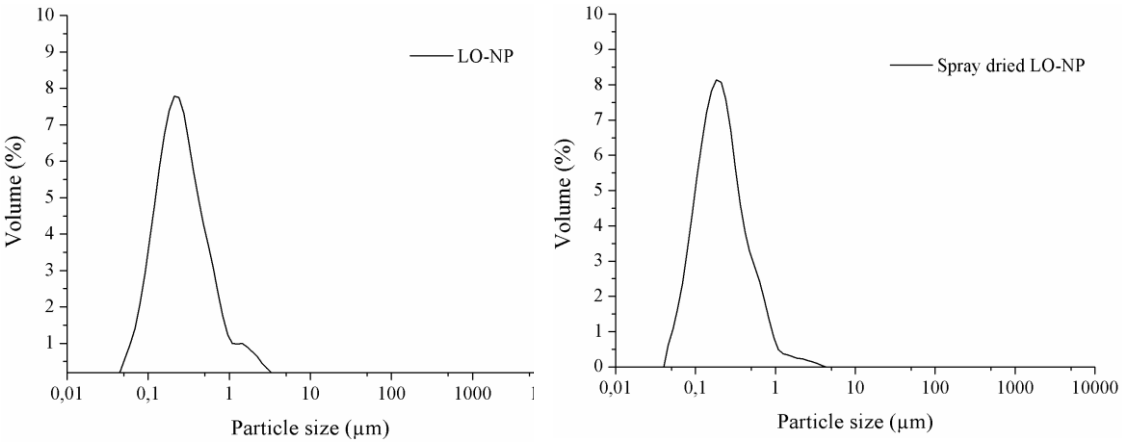

Fig. 5. Particle size distribution curves of LO-NP and spray dryed LO-NP.

3.8 Physicochemical characterization of orange juice enriched with LO-NP

The results of total soluble solids, pH, titratable acidity and color measurements for orange juice and orange juice with LO-NP are shown in Table 2. No significant difference was observed between pH and TA measured in orange juice and orange juice with LO-NP. The TSS was higher in orange juice with LO-NP, due to the presence of LO-NP powder in the juice.

Juice color is an important factor that influences consumer sensory acceptance. The color measurements showed that orange juice with LO-NP presented significantly higher values for lightness (L*) and lower values for red-green intensity (a*). These difference may be due to the presence of CSM, oil and Tween 80® in the juice, which would give greater luminosity and slight increase in red intensity due to the color of LO-NP. The yellow-blue intensity (b*) had no significant difference between orange juice and orange juice with LO-NP.

A evaluation of untreated pure orange juice used as control group by (Tiwari, Muthukumarappan, O'Donnell, & Cullen, 2008) and (Cortés, Esteve, & Frígola, 2008) related higher values for color measurements of orange juice: L* 59.71, a* 7.44, b* 56.29 and L* 51.36, a*, 4.56, b* 50.73 respectively. These differences may be due to the type and place of fruit cultivation, juice processing and time and storage conditions.

Table 2. Physicochemical characterization of orange juice and orange juice enriched with LO-NP.

	Orange juice	Orange juice with LO-NP
Titratable acidity	1.43 ± 0.02[a]	1.46 ± 0.02[a]
Hydrogen potential	3.28 ± 0.07 [a]	3.24 ± 0.02 [a]
Total soluble solids	10.54 % ± 0.002 [b]	12.14 % ± 0.001 [a]
Color co-ordinate a*	- 0.98 ± 0.07[a]	- 1.33 ± 0.09[b]
Color co-ordinate b*	15.92 ± 0.07[a]	16.00 ± 0.13[a]

Color co-ordinate L*	42.55 ± 0.03[b]	43.93 ± 0.25[a]

The results are represented as the means ± standard desviation (n = 3).Values within each line with the same letter are not significantly different (p > 0,05).

3.9 Sensory evaluation

The atributes appearance, color, flavor, texture, taste, aftertaste and overall acceptability of orange juice with LO-NP evaluated through sensory analyses are represented in Fig. 6.

The two orange juice samples (pure orange juice and orange juice with addition of LO-NP powder) showed no significant difference among the evaluated parameters. The high solubility of spray-dried LO-NP is the most likely cause of the lack of differences between pure orange juice and orange juice enriched with LO-NP. The overall acceptability of the orange juice with LO-NP was 83 %, indicating that the enrichment of orange juice with spray-dried LO-NP did not affect sensorial acceptability. According to (Habibi, Keramat, Hojjatoleslamy, & Tamjidi, 2017) pomegranate juice fortified with powder of microencapsulated fish oil within the complex coacervates of gelatin–gum arabic showed a considerable decrease in its sensorial acceptability. (Tamjidi, Nasirpour, & Shahedi, 2012) showed that microencapsulated fish oil powder added to milk improved sensorial parameters of manufactured enriched yogurt.

As the difference between the two juices was not perceived, it is feasible to add the nanoparticles to orange juice enrichment, without significant sensorial difference.

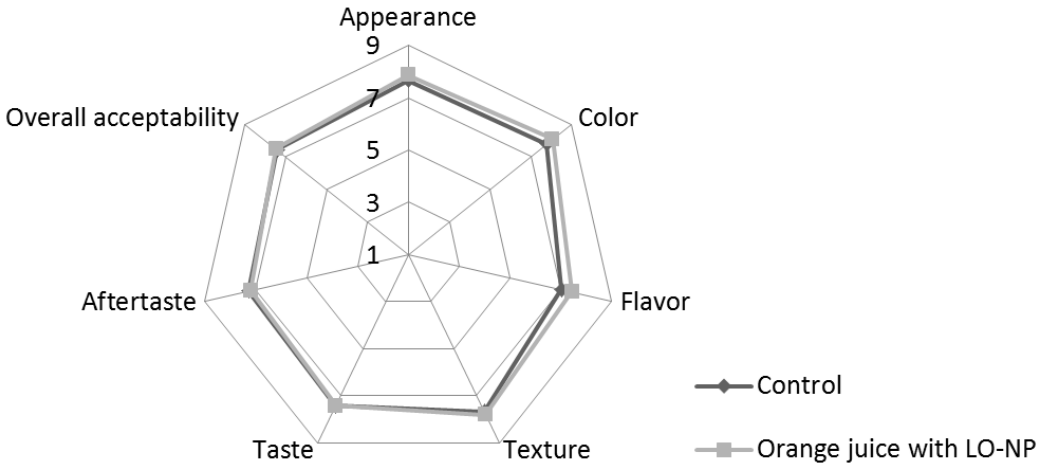

Fig 6. – Sensory analysis scores of orange juice and orange juice with LO-NP.

4. Conclusion

The results found in this study showed that chia mucilage is a good wall material to substitute synthetic polymers in the nanoencapsulation process andthe enrichment of orange juice with linseed oil can be achieved by LO nanoencapsulation with chia mucilage and subsequent spray-drying process, increasing oil solubility. Further assays are required to evaluate in vitro digestion parameters to predict the digestion behavior of LO-NP.

5. References

Baboota, S., Rahman, M. u., Kumar, A., Sharma, S., Sahni, J., & Ali, J. (2012). Submicron Size Formulation of Linseed Oil Containing Omega-3 Fatty Acid for Topical Delivery. *Journal of Dispersion Science and Technology, 33*(9), 1259-1266. doi:10.1080/01932691.2011.596339

Bustamante, M., Oomah, B. D., Rubilar, M., & Shene, C. (2017). Effective Lactobacillus plantarum and Bifidobacterium infantis encapsulation with chia seed (Salvia hispanica L.) and flaxseed (Linum usitatissimum L.) mucilage and soluble protein by spray drying. *Food Chemistry, 216*, 97-105. doi:http://dx.doi.org/10.1016/j.foodchem.2016.08.019

Cortés, C., Esteve, M. J., & Frígola, A. (2008). Color of orange juice treated by High Intensity Pulsed Electric Fields during refrigerated storage and comparison with pasteurized juice. *Food Control, 19*(2), 151-158. doi:http://dx.doi.org/10.1016/j.foodcont.2007.03.001

Dawczynski, C., Martin, L., Wagner, A., & Jahreis, G. (2010). n-3 LC-PUFA-enriched dairy products are able to reduce cardiovascular risk factors: a double-blind, cross-over study. *Clin Nutr, 29*(5), 592-599. doi:10.1016/j.clnu.2010.02.008

de Campo, C., dos Santos, P. P., Costa, T. M. H., Paese, K., Guterres, S. S., Rios, A. d. O., & Flôres, S. H. (2017). Nanoencapsulation of chia seed oil with chia mucilage (Salvia hispanica L.) as wall material: Characterization and stability evaluation. *Food Chemistry, 234*, 1-9. doi:https://doi.org/10.1016/j.foodchem.2017.04.153

de Oliveira, E. F., Paula, H. C. B., & Paula, R. C. M. d. (2014). Alginate/cashew gum nanoparticles for essential oil encapsulation. *Colloids and Surfaces B: Biointerfaces, 113*, 146-151. doi:https://doi.org/10.1016/j.colsurfb.2013.08.038

Dick, M., Costa, T. M. H., Gomaa, A., Subirade, M., Rios, A. d. O., & Flôres, S. H. (2015). Edible film production from chia seed mucilage: Effect of glycerol concentration on its physicochemical and mechanical properties. *Carbohydrate Polymers, 130*, 198-205. doi:http://dx.doi.org/10.1016/j.carbpol.2015.05.040

Dickinson, E. (2006). *Food Hydrocolloids, 20*(1), 137. doi:http://dx.doi.org/10.1016/j.foodhyd.2005.05.001

dos Santos, P. P., Paese, K., Guterres, S. S., Pohlmann, A. R., Costa, T. H., Jablonski, A., . . . Rios, A. d. O. (2015). Development of lycopene-loaded lipid-core nanocapsules: physicochemical characterization and stability study. *Journal of Nanoparticle Research, 17*(2), 107. doi:10.1007/s11051-015-2917-5

Duan, X., Tian, X., Ke, J., Yin, Y., Zheng, J., Chen, J., . . . Yuan, Y. (2016). Size controllable redispersion of sintered Au nanoparticles by using iodohydrocarbon and its implications. *Chemical Science, 7*(5), 3181-3187. doi:10.1039/C5SC04283F

El-Beltagi, H., Salama, Z., & El-Hariri, D. (2007). Evaluation of fatty acids profile and the content of some secondary metabolites in seeds of different flax cultivars (Linum usitatissimum L.). *General and Applied Plant Physiology, 33*(3-4), 187-202.

Flores, F. C., Ribeiro, R. F., Ourique, A. F., Rolim, C. M. B., Silva, C. d. B. d., Pohlmann, A. R., . . . Guterres, S. S. (2011). Nanostructured systems containing an essential oil: protection against volatilization. *Química Nova, 34*, 968-972.

Gallardo, G., Guida, L., Martinez, V., López, M. C., Bernhardt, D., Blasco, R., . . . Hermida, L. G. (2013). Microencapsulation of linseed oil by spray drying for functional food application. *Food Research International, 52*(2), 473-482. doi:https://doi.org/10.1016/j.foodres.2013.01.020

Ganta, S., & Amiji, M. (2009). Coadministration of Paclitaxel and Curcumin in Nanoemulsion Formulations To Overcome Multidrug Resistance in Tumor Cells. *Molecular Pharmaceutics, 6*(3), 928-939. doi:10.1021/mp800240j

Gittings, M. R., & Saville, D. A. (1998). The determination of hydrodynamic size and zeta potential from electrophoretic mobility and light scattering measurements. *Colloids and Surfaces A: Physicochemical and Engineering Aspects, 141*(1), 111-117. doi:http://dx.doi.org/10.1016/S0927-7757(98)00207-6

Goh, K. K. T., Matia-Merino, L., Chiang, J. H., Quek, R., Soh, S. J. B., & Lentle, R. G. (2016). The physico-chemical properties of chia seed polysaccharide and its microgel dispersion rheology. *Carbohydrate Polymers, 149*, 297-307. doi:http://dx.doi.org/10.1016/j.carbpol.2016.04.126

González, A., Martínez, M. L., Paredes, A. J., León, A. E., & Ribotta, P. D. (2016). Study of the preparation process and variation of wall components in chia (Salvia hispanica L.) oil microencapsulation. *Powder Technology, 301*, 868-875. doi:http://dx.doi.org/10.1016/j.powtec.2016.07.026

Gouin, S. (2004). Microencapsulation. *Trends in Food Science & Technology, 15*(7), 330-347. doi:http://dx.doi.org/10.1016/j.tifs.2003.10.005

Guillén, M. D., & Ruiz, A. (2005). Oxidation process of oils with high content of linoleic acyl groups and formation of toxic hydroperoxy- and hydroxyalkenals. A study by 1H nuclear magnetic resonance. *Journal of the Science of Food and Agriculture, 85*(14), 2413-2420. doi:10.1002/jsfa.2273

Habibi, A., Keramat, J., Hojjatoleslamy, M., & Tamjidi, F. (2017). Preparation of Fish Oil Microcapsules by Complex Coacervation of Gelatin–Gum Arabic and their Utilization for Fortification of Pomegranate Juice. *Journal of Food Process Engineering, 40*(2), n/a-n/a. doi:10.1111/jfpe.12385

Hayes, P. A., Vahur, S., & Leito, I. (2014). ATR-FTIR spectroscopy and quantitative multivariate analysis of paints and coating materials. *Spectrochimica Acta Part A: Molecular and Biomolecular Spectroscopy, 133*, 207-213. doi:http://dx.doi.org/10.1016/j.saa.2014.05.058

Herculano, E. D., de Paula, H. C. B., de Figueiredo, E. A. T., Dias, F. G. B., & Pereira, V. d. A. (2015). Physicochemical and antimicrobial properties of nanoencapsulated Eucalyptus staigeriana essential oil. *LWT - Food Science and Technology, 61*(2), 484-491. doi:http://dx.doi.org/10.1016/j.lwt.2014.12.001

Ilyasoglu, H., & El, S. N. (2014). Nanoencapsulation of EPA/DHA with sodium caseinate–gum arabic complex and its usage in the enrichment of fruit juice. *LWT - Food Science and Technology, 56*(2), 461-468. doi:http://dx.doi.org/10.1016/j.lwt.2013.12.002

Joseph, J. D., & Ackman, R. G. (1992). Capillary column gas chromatographic method for analysis of encapsulated fish oils and fish oil ethyl esters: collaborative study. *Journal of AOAC International, 75*(3), 488-506.

Khoshakhlagh, K., Koocheki, A., Mohebbi, M., & Allafchian, A. (2017). Development and characterization of electrosprayed Alyssum homolocarpum seed gum nanoparticles for encapsulation of d-limonene. *Journal of Colloid and Interface Science, 490*, 562-575. doi:http://dx.doi.org/10.1016/j.jcis.2016.11.067

Kolanowski, W., & Weißbrodt, J. (2007). Sensory quality of dairy products fortified with fish oil. *International Dairy Journal, 17*(10), 1248-1253. doi:https://doi.org/10.1016/j.idairyj.2007.04.005

Martínez, M. L., Curti, M. I., Roccia, P., Llabot, J. M., Penci, M. C., Bodoira, R. M., & Ribotta, P. D. (2015). Oxidative stability of walnut (Juglans regia L.) and chia (Salvia hispanica L.) oils microencapsulated by spray drying. *Powder Technology, 270*, 271-277. doi:http://dx.doi.org/10.1016/j.powtec.2014.10.031

Meilgaard, M., Civille, G. V., & Caar, B. T. (2007). *Sensory Evaluation Techniques.* (B. R. C. Press. Ed.).

Naji-Tabasi, S., & Razavi, S. M. A. (2017). Functional properties and applications of basil seed gum: An overview. *Food Hydrocolloids*. doi:http://dx.doi.org/10.1016/j.foodhyd.2017.07.007

Popa, V.-M., Gruia, A., Raba, D., Dumbrava, D., Moldovan, C., Bordean, D., & Mateescu, C. (2012). Fatty acids composition and oil characteristics of linseed (Linum Usitatissimum L.) from Romania. *Journal of Agroalimentary Processes and Technologies, 18*(2), 136-140.

Prajapati, V. D., Jani, G. K., Moradiya, N. G., & Randeria, N. P. (2013). Pharmaceutical applications of various natural gums, mucilages and their modified forms. *Carbohydrate Polymers, 92*(2), 1685-1699. doi:http://dx.doi.org/10.1016/j.carbpol.2012.11.021

Rocha, A. M. C. N., & Morais, A. M. M. B. (2003). Shelf life of minimally processed apple (cv. Jonagored) determined by colour changes. *Food Control, 14*(1), 13-20. doi:http://dx.doi.org/10.1016/S0956-7135(02)00046-4

Sarika, P. R., Pavithran, A., & James, N. R. (2015). Cationized gelatin/gum arabic polyelectrolyte complex: Study of electrostatic interactions. *Food Hydrocolloids, 49*, 176-182. doi:http://dx.doi.org/10.1016/j.foodhyd.2015.02.039

Silverstein, R. M., Webster, F. X., & Kiemle, D. J. (2007). *Identificação Espectrométrica de Compostos Orgânicos* . (N. Y. S. U. o. N. York Ed. College of Environmental Science & Forestry ed.).

Tamjidi, F., Nasirpour, A., & Shahedi, M. (2012). Physicochemical and sensory properties of yogurt enriched with microencapsulated fish oil. *Food Sci Technol Int, 18*(4), 381-390. doi:10.1177/1082013211428212

Timilsena, Y. P., Wang, B., Adhikari, R., & Adhikari, B. (2016). Preparation and characterization of chia seed protein isolate–chia seed gum complex coacervates. *Food Hydrocolloids, 52*, 554-563. doi:http://dx.doi.org/10.1016/j.foodhyd.2015.07.033

Tiwari, B. K., Muthukumarappan, K., O'Donnell, C. P., & Cullen, P. J. (2008). Colour degradation and quality parameters of sonicated orange juice using response surface methodology. *LWT - Food Science and Technology, 41*(10), 1876-1883. doi:http://dx.doi.org/10.1016/j.lwt.2007.11.016

Us-Medina, U., Ruiz-Ruiz, J. C., Quintana-Owen, P., & Segura-Campos, M. R. (2017). Salvia hispanica mucilage-alginate properties and performance as an encapsulation matrix for chia seed oil. *Journal of Food Processing and Preservation*, n/a-n/a. doi:10.1111/jfpp.13270

Wongsagonsup, R., Shobsngob, S., Oonkhanond, B., & Varavinit, S. (2005). Zeta Potential (ζ) Analysis for the Determination of Protein Content in Rice Flour. *Starch - Stärke, 57*(1), 25-31. doi:10.1002/star.200400307